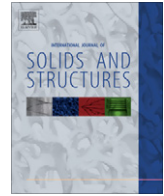


Contents lists available at [SciVerse ScienceDirect](http://www.sciencedirect.com)

International Journal of Solids and Structures

journal homepage: www.elsevier.com/locate/ijsolstr

Hierarchical honeycombs with tailorable properties

Amin Ajdari, Babak Haghpanah Jahromi, Jim Papadopoulos, Hamid Nayeb-Hashemi, Ashkan Vaziri*

Department of Mechanical and Industrial Engineering, Northeastern University, Boston, MA, United States

ARTICLE INFO

Article history:

Received 22 October 2011

Received in revised form 19 January 2012

Available online xxx

Keywords:

Structural hierarchy

Honeycombs

Cellular structures

ABSTRACT

We investigated the mechanical behavior of two-dimensional hierarchical honeycomb structures using analytical, numerical and experimental methods. Hierarchical honeycombs were constructed by replacing every three-edge vertex of a regular hexagonal lattice with a smaller hexagon. Repeating this process builds a fractal-appearing structure. The resulting isotropic in-plane elastic properties (effective elastic modulus and Poisson's ratio) of this structure are controlled by the dimension ratios for different hierarchical orders. Hierarchical honeycombs of first and second order can be up to 2.0 and 3.5 times stiffer than regular honeycomb at the same mass (i.e., same overall average density). The Poisson's ratio varies from nearly 1.0 (when planar 'bulk' modulus is considerably greater than Young's modulus, so the structure acts 'incompressible' for most loadings) to 0.28, depending on the dimension ratios. The work provides insight into the role of structural organization and hierarchy in regulating the mechanical behavior of materials, and new opportunities for developing low-weight cellular structures with tailorable properties.

© 2012 Elsevier Ltd. All rights reserved.

1. Introduction

Hierarchical structures are ubiquitous in nature and can be observed at many different scales in organic materials and biological systems (Aizenberg et al., 2005; Buehler, 2006; Espinosa et al., 2011; Fratzi and Weinkamer, 2007; Gibson et al., 2010; Lakes, 1993; Ortiz and Boyce, 2008; Qing and Mishnaevsky Jr, 2009). The hierarchical organization of these systems generally plays a key role in their properties, function and survival (Fratzi and Weinkamer, 2007; Gibson et al., 2010). Hierarchy is also important in engineering designs, materials and architecture. Examples range from the Eiffel tower (Lakes, 1993) and polymers with micro-level hierarchical structures (Lakes, 1993), to sandwich panels with cores made of foams or composite lattice structures (Cote et al., 2009; Fan et al., 2008; Kazemahvazi et al., 2009; Kazemahvazi and Zenkert, 2009; Kooistra et al., 2007). There, the hierarchical organization can lead to superior mechanical behavior and tailorable properties, as described recently for sandwich cores with hierarchical structure (Fan et al., 2008) and for hierarchical corrugated truss structures (Kooistra et al., 2007). The overall mechanical behavior of these structures is governed by the response at different length scales and levels of hierarchy; and increasing levels of structural hierarchy can result in lighter-weight and better-performing structures (Bhat et al., 1989; Burgueño et al., 2005;

Gibson et al., 2010; Kooistra et al., 2007; Lakes, 1993; Murphey and Hinkle, 2003; Taylor et al., 2011).

Here, we have presented a systematic way to incorporate hierarchy in honeycomb structures. Honeycombs are two-dimensional cellular structures used in different applications including thermal isolation (Lu and Chen, 1999), impact energy absorption and structural protection (Ajdari et al., 2011; Vaziri et al., 2007; Wadley et al., 2007; Vaziri and Xue, 2007; Zheng et al., 2005), and as the core of lightweight sandwich panels (Vaziri and Hutchinson, 2007; Rathbun et al., 2006; Vaziri et al., 2006; Xue and Hutchinson, 2006), Xue and Hutchinson, 2004. The transverse (i.e., in-plane) stiffness and strength of honeycombs are generally governed by the bending deformation of cell walls, and strongly depend on the honeycomb relative density (Gibson and Ashby, 1997). Under uniform transverse loading, the maximum bending moment in each cell wall occurs at the honeycomb vertices (i.e., cell wall corners). Thus, moving material from the middle part of each wall closer to the vertices can potentially increase the transverse stiffness and strength (Chuang and Huang, 2002a,b; Simone and Gibson, 1998). Here, we replace the vertices of a regular hexagonal lattice with smaller hexagons (simultaneously reducing the wall thickness to maintain fixed overall density), to achieve a structure with one level of hierarchy. This will be shown able to exhibit a Young's modulus superior to that of its regular hexagonal counterpart of equal relative density. This replacement procedure for three-edge vertices can be repeated at smaller scales to achieve fractal-appearing honeycombs with higher orders of structural hierarchy. Fig. 1(A) shows the evolution of a hexagonal honeycomb cell as structural hierarchy is increased. The structural organization of

* Corresponding author. Tel.: +1 617 373 3474; fax: +1 617 495 9837.

E-mail address: vaziri@coe.neu.edu (A. Vaziri).

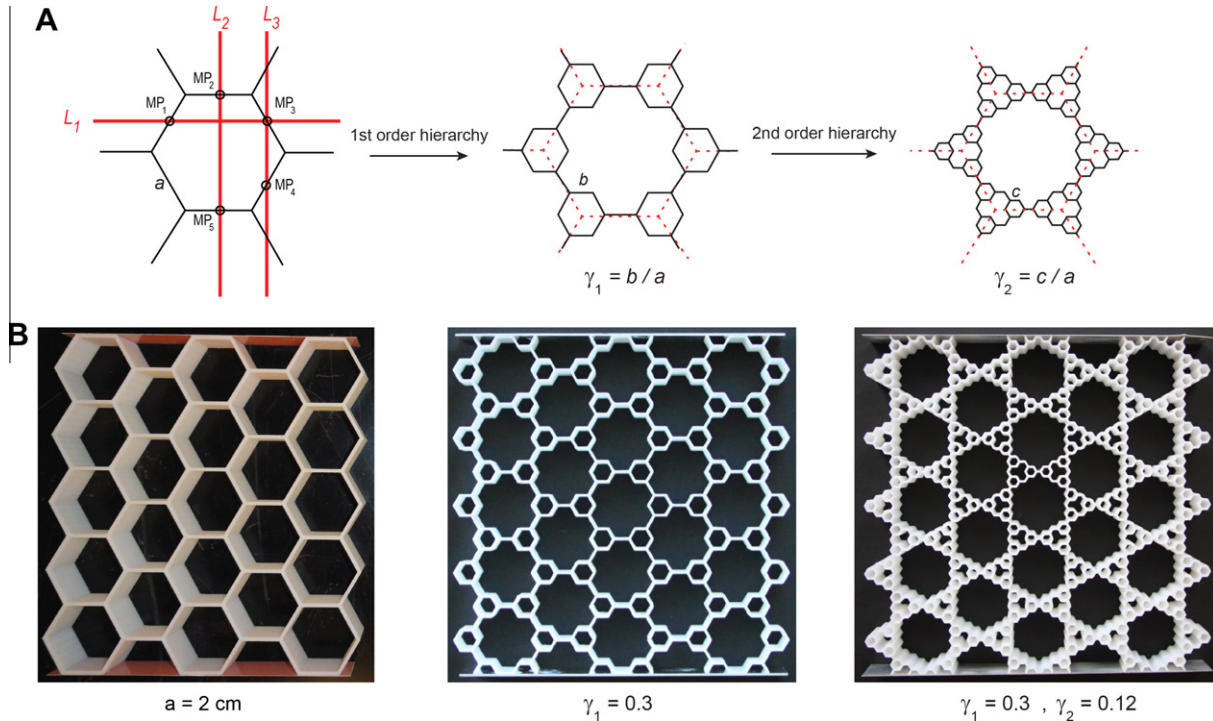


Fig. 1. Hierarchical honeycombs. (A) Unit cell of the hierarchical honeycombs with regular structure and with 1st and 2nd order hierarchy. (B) Images of honeycombs with $a = 2$ cm fabricated using three-dimensional printing.

the honeycomb at each level of hierarchy can be defined by the ratio of the introduced hexagonal edge length (b for 1st order hierarchy and c for 2nd order hierarchy), to the original hexagon's edge length, a , as described in Fig. 1(A) (i.e., $\gamma_1 = b/a$ and $\gamma_2 = c/a$). For a honeycomb with 1st order hierarchy, $0 \leq b \leq a/2$ and thus, $0 \leq \gamma_1 \leq 0.5$, where $\gamma_1 = 0$ denotes the regular honeycomb structure. For a honeycomb with 2nd order hierarchy, there are two geometrical constraints, $0 \leq c \leq b$ and $c \leq a/2 - b$. In terms of the ratio parameters, the constraints are $0 \leq \gamma_2 \leq \gamma_1$ if $\gamma_1 \leq 0.25$ and $0 \leq \gamma_2 \leq (0.5 - \gamma_1)$ if $0.25 \leq \gamma_1 \leq 0.5$. The dimensionless relative density (i.e., area fraction), can be given in terms of t/a :

$$\rho = 2\sqrt{3} \cdot (1 + 2\gamma_1 + 6\gamma_2) \cdot t/a, \quad (1)$$

where t is the thickness of the cell walls, from which the special cases of γ_2 , $\gamma_1 = 0$ can be read off immediately. (For regular honeycomb, $\rho = 2/\sqrt{3} \cdot 2/t/a$; and for honeycomb with 1st order hierarchy, $\rho = 2\sqrt{3} \cdot (1 + 2\gamma_1) \cdot t/a$). This relation clearly shows that t/a must decrease to maintain fixed relative density as γ_1 , γ_2 are increased.

Here, we studied the effective elastic properties hierarchical honeycombs using analytical, numerical and experimental methods. The hierarchical honeycomb samples were fabricated using 3D printing as discussed in Section 2. In Sections 3 and 4, we provided analytical models to estimate the effective elastic modulus and Poisson's ratio of hierarchical honeycombs using the concepts of mechanics of materials and compare the analytical results with finite element simulations and experiments. In Section 5, we summarized the elastic properties of the hierarchical honeycombs and draw conclusions, while discussing additional possibilities for further enhancement of the performance of hierarchical honeycombs.

2. Fabrication using 3D printing

Fig. 1(B) shows samples of regular and hierarchical honeycombs with $\rho = 0.10$ and $a = 20$ mm fabricated using 3D printing (Dimensions 3D printer, Stratasys Inc., Eden Prairie, MN). The

regular honeycomb has $t = 1.75$ mm; the honeycomb with one-level hierarchy has $\gamma_1 = 0.3$ and $t = 1$ mm; and that with two-level hierarchy has $\gamma_1 = 0.3$, $\gamma_2 = 0.12$, and $t = 0.75$ mm. These were printed as three-dimensional extruded shells from an ABS polymer (acrylonitrile butadiene styrene, elastic modulus = 2.3 GPa) as the bulk material. The input file to the 3D printing software was created for honeycombs with a relative density of 0.10. The cell wall thickness was reduced for honeycombs with hierarchy in order to keep the overall relative density constant, similar to the finite element calculations. The actual printed samples did not maintain the target density very precisely due to the 0.25 mm resolution of the printer (so the relative density was between 8–12%, and only certain discrete values of γ_1 and γ_2 could be achieved). Prior to the experiments, aluminum plates were bonded to the top and bottom of the samples using cyanoacrylate adhesive, in order to prevent the edge nodes (similar to 1, 2, 3, and 4 in Fig. 2(A) from excessive bending. The in-plane compressive response of these bonded-end samples was measured using an INSTRON 5582 at the slow rate of 1mm/min (i.e., strain rate, $\dot{\epsilon} = 0.5\%/min$). The effective elastic modulus of the honeycombs were estimated from the slope of the force-displacement curve at early stage of the experiment ($\epsilon < 1.5\%$). For each specimen, the true relative density was measured by weighing, and then was used when calculating the normalized effective elastic modulus. For each configuration, three samples were tested. In addition to the experiments, we developed analytical and finite element models to calculate the effective in-plane elastic constants of the honeycombs in terms of cell-wall Young's modulus.

3. Hierarchical honeycombs: effective elastic modulus

For the analytical approach, we used Castigliano's second theorem (Boresi and Schmidt, 2002) to determine the uniaxial in-plane deformation of hierarchical honeycombs made of an isotropic elastic material with elastic modulus, E_s . It is well known that plane

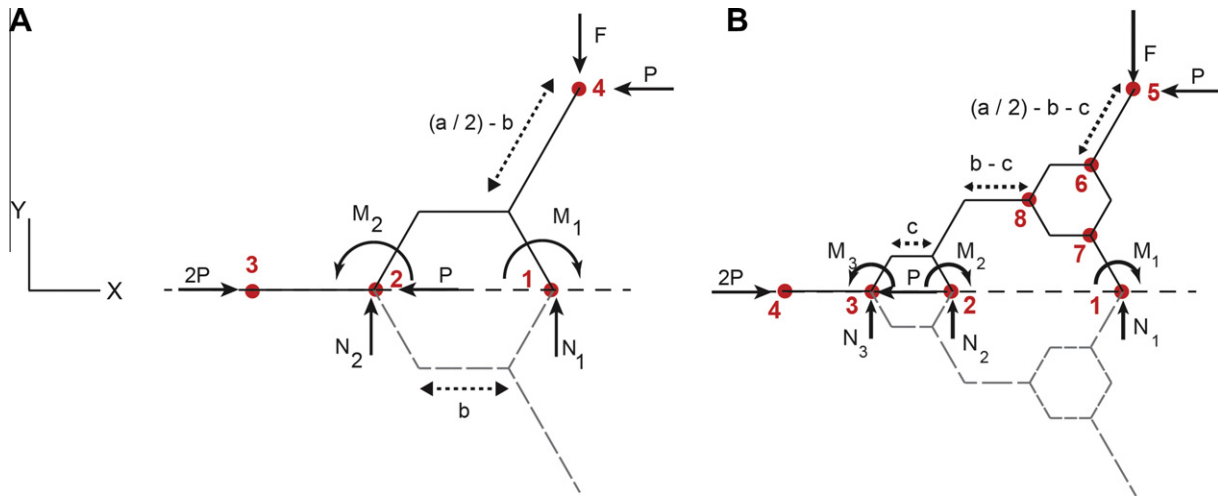


Fig. 2. Free body diagrams of the subassembly of honeycombs with 1st and 2nd order hierarchy used in the analytical estimation. N_i and M_i ($i = 1$ to 3) denote the reaction vertical forces and moments in the nodes of the subassembly structures as denoted in the pictures. It should be noted that P is not an actual load, it is rather a dummy force so Castigliano's method can be used for horizontal strain.

lattices with threefold symmetry will exhibit macroscopically isotropic in-plane elastic behavior (Christensen, 1987). Thus, the macroscopic in-plane linear elastic behavior of hierarchical honeycomb can be characterized by just two constants, to be found by whatever loadings are most convenient. We imposed a far field y -direction stress, $\sigma_{yy} = -(2/3)F/a$, in a vertical direction (perpendicular to the horizontal hexagon edges in Fig. 1(A)). This is equivalent to applying a vertical force F at every cut-point of a horizontal line (such as L_1 in Fig. 1A) passing through the mid-points of non-horizontal edges in a row of underlying (i.e., no hierarchy) hexagons.

To understand the analysis, it is helpful to envision the underlying regular hexagonal network as illustrated in Fig. 1(A). Midpoints of various edges have been labeled MP_1 to MP_5 . For a macroscopic state of stress σ_{ij} , the average force per unit length transmitted across a vertical line such as L_2 is σ_{11} (direct) and σ_{12} (shear). Since only σ_{22} is nonzero, no net horizontal or vertical force is transmitted across L_2 . Yet every horizontal bar is equivalent, allowing us to conclude that they transmit neither axial nor shear force. Furthermore, they also transmit no bending moment, because a consistent moment, such as sagging, it would break the symmetry about horizontal lines. Therefore, the horizontal cut by L_2 are entirely load-free for this state of stress.

Next, considering the edges cut at their midpoints by line L_1 , it was already stated that each cut bar must sustain a vertical force $F = -3\sigma_{yy}a/2$. Cut at the midpoints as they are, we can conclude that no bending moment is transmitted by these bars, because that would imply a bar curvature or 'bulging' in a way prohibited by symmetry. (For example, if the bar at MP_3 is bulged 'outward', horizontal and vertical reflection symmetry would mean that all four non-horizontal bars of the base hexagon are bulged outward. But the bar at MP_3 is shared by an adjacent hexagon, which should similarly bulge outward – an inconsistency.)

Since $\sigma_{12} = 0$, no net horizontal force is transmitted across L_1 . Therefore, considering the structure below L_1 , a leftward force applied to MP_3 balanced by a rightward force at MP_1 might be envisaged. But by reflection in a horizontal line through the hexagon center, we would also have to expect a leftward force applied to the bar above a cut at MP_4 . The resulting net leftward force on the bars between cuts at MP_3 and MP_4 is not possible because we already know that the horizontal bars (e.g., on the line through the hexagon center) are tension-free. We can thus conclude that the forces at cut points MP_1 , MP_3 , and MP_4 are purely vertical with magnitude F . This 'hexagon midpoint' reasoning is unchanged when structural hierarchy is introduced.

Fig. 2(A) shows the free body diagram of a subassembly able to represent an entire honeycomb with 1st order hierarchy subject to σ_{yy} loading (therefore, for this section, to find effective elastic modulus in y -direction, we are not taking the horizontal forces shown at point 2, 3, and 4 into account – It should be noted that the horizontal forces shown in the figures are not an actual load, it is rather a dummy force so Castigliano's method can be used for horizontal strain.) According to the above arguments, 3 is load-free, and 4 is subject only to force $-F$ in the y direction. Since the subassembly is also cut free at points 1 and 2, we need to find the force and moment reactions at those cuts. y -direction forces acting on the subassembly are denoted by N_1 and N_2 , and moments are denoted by M_1 and M_2 . There can be no horizontal force at point 1 because of reflection symmetry about the x axis, along with the lack of any third force on point 1 to balance same-direction horizontal inputs from above and below. At point 2, since no other horizontal forces act on the subassembly, we can also be sure that there is no horizontal reaction. So in this problem, x -direction equilibrium is trivially satisfied. By applying the y -force and moment balance laws to the subassembly, N_2 and M_2 can therefore be written as linear functions of N_1 , M_1 , and F . The bending energy stored in the subassembly can be expressed as a sum over all the beams: $U(F, M_1, N_1) = \sum \int (M^2)/(2E_s I) ds$, where M is the bending moment at location s along the beam, E_s is the elastic modulus of the cell wall material, and I is the beam's cross sectional area moment of inertia at s (cell walls are considered to have rectangular cross section with thickness, t , and unit depth; i.e., $I = t^3/12$). Since the beam resultants are linear in F , M_1 and N_1 , U is then a quadratic function of those same quantities. The horizontal beam connecting nodes 2 and 3 can be excluded from the analysis since it is load-free.

Since there is zero vertical displacement and zero rotation at point 1 due to symmetry, we can use Castigliano's method to write $\partial U/\partial N_1 = 0$, and $\partial U/\partial M_1 = 0$. These two relations allow N_1 and M_1 to be calculated in terms of F : $N_1 = F(0.533 + 0.15/\gamma_1)$, $M_1 = Fa(0.283\gamma_1 - 0.017)$. At point 4 we can find the displacement $\delta = \partial U/\partial F$, and then the above substitution for N_1 and M_1 gives $\delta = \sqrt{3}Fa^3/(72E_s I f(\gamma_1))$. The effective elastic modulus (to be normalized by beam material modulus, E_s) is then defined as the ratio of average stress ($-2F/3a$) and average strain, ($-4\delta/a\sqrt{3}$):

$$E/E_s = (t/a)^3 f(\gamma_1) \tag{2}$$

where $f(\gamma_1) = \sqrt{3}/(0.75 - 3.525\gamma_1 + 3.6\gamma_1^2 + 2.9\gamma_1^3)$. To find the maximum normalized elastic modulus for structures with

first-level hierarchy and constant relative density, we eliminate (t/a) from Eq. (2) by using the relative density expression of Eq. (1). The resulting expression for E/E_s is ρ^3 times a function of γ_1 , and setting $(\partial(E/E_s)/\partial\gamma_1)_\rho = 0$ gives $\gamma_1 = 0.32$. Making this substitution leads to $E/E_s = 2.97\rho^3$, a stiffness almost twice the stiffness of the regular honeycomb structure (Gibson and Ashby, 1997), for which $E_0/E_s = 1.5\rho^3$. (The regular honeycomb result can be found by letting $\gamma_1 = 0$ in Eq. (2), and using Eq. (1) to eliminate t/a).

The same analytical approach was used to evaluate the in-plane effective Young's modulus of honeycomb with two orders of hierarchy, as a function of hierarchy indices γ_1 and γ_2 . Fig. 2(B) shows the free body diagram of a subassembly chosen to minimize calculation. As before, the vertical compressive stress ($-2F/3a$) is achieved by the external force, F , applied downward at point 5 (a midpoint of the underlying hexagon side), with symmetry arguments showing that no other loads act at that point. Bar 3–4 is again load-free. The same argument applies to point 3 as formerly applied to point 2 for the honeycomb with one order of hierarchy. And, the same argument applies to points 2 and 1 as formerly applied to point 1. Therefore, N_1, M_1, N_2, M_2, N_3 , and M_3 are the unknown reaction forces and moments at vertices 1, 2, and 3 as shown in Fig. 2(B). One additional step required for analysis of the second-order hierarchy is to determine the beam resultants for the statically indeterminate, complete (small) hexagon of side c embedded in each subassembly, loaded at nodes 6 and 7 with reactions at node 8. The bending moments along each side of the c-hexagon are determined from a subsidiary analysis in which it is divided at nodes 6 and 7, and then three compatibility conditions are enforced at each of those nodes. The details of that analysis are omitted for brevity. Similar to honeycombs with first order hierarchy, using the y-direction and rotational equilibrium equations, N_3 and M_3 can be written as a function of N_1, M_1, N_2, M_2 , and F . Therefore, the total energy of the investigated substructure, which is the sum of the bending strain energy of all the beams, can be written as: $U(F, M_1, N_1, M_2, N_2) = \sum \int (M^2/(2E_s I)) ds$. The following four boundary conditions are imposed at points 1 and 2 to achieve the zero rotation and zero displacement demanded by symmetry, as shown in Fig. 2(B): $\partial U/\partial N_1 = 0, \partial U/\partial M_1 = 0, \partial U/\partial N_2 = 0$, and $\partial U/\partial M_2 = 0$. These relations allow us to solve for M_1, N_1, M_2, N_2 . In a similar way as above the effective elastic modulus can be presented as:

$$E/E_s = (t/a)^3 f(\gamma_1, \xi) \quad (3)$$

where $\xi = \gamma_2/\gamma_1$ and $f(\gamma_1, \xi) = N_4(\xi)/(\gamma_1^3 D_7(\xi)) + \gamma_1^2 D_6(\xi) + \gamma_1 D_5(\xi) + D_4(\xi)$

$$N_4(\xi) = 29.62 - 54.26\xi + 31.75\xi^2 - 4.73\xi^3 - \xi^4$$

$$D_7(\xi) = 49.64 - 609.01\xi + 862.56\xi^2 - 195.50\xi^3 - 270.14\xi^4 \\ + 159.95\xi^5 - 18.13\xi^6 - 2.20\xi^7$$

$$D_6(\xi) = 61.73 + 310.43\xi - 662.32\xi^2 + 334.12\xi^3 + 9.70\xi^4 \\ - 29.38\xi^5 - 1.88\xi^6$$

$$D_5(\xi) = 60.43 + 12.80\xi + 123.22\xi^2 - 108.06\xi^3 + 20.50\xi^4 + 3.90\xi^5$$

$$D_4(\xi) = 12.80 - 23.46\xi + 13.74\xi^2 + 2.04\xi^3 - 0.43\xi^4$$

For the 2nd order hierarchical structure, once again eliminating (t/a) in favor of density, and then differentiating at constant density, $(\partial(E/E_s)/\partial\gamma_1)_\rho = (\partial(E/E_s)/\partial\gamma_2)_\rho = 0$ give $\gamma_1 = 0.32$, and $\gamma_2 = 0.135$, leading to $E/E_s = 5.26\rho^3$, a stiffness almost 3.5 times that of the regular honeycomb.

To validate the theoretical results we simulated the structural response using finite element analysis. Two-dimensional hierarchical honeycombs were modeled using Abaqus 6.10 (SIMULIA, Providence, RI). All models were meshed using the BEAM22 element, which is capable of capturing not only the bending compliance of the above theory, but also the axial and shear deformations which may become significant at greater values of t/a . A rectangular cross section with unit length normal to the plane of loading was assumed for the cell wall beams. The thickness of all the beams was adjusted to control the overall relative density of the structure. The material properties of aluminum, $E_s = 70$ GPa, and $\nu_s = 0.3$, were used in this study. We performed the analysis with two different boundary conditions representing our analytical model and experimental tests, respectively. In the first set, we applied periodic boundary conditions to matching nodes on the left and right edges, as if the sample were infinitely wide but free to strain laterally (Harders et al., 2005). To model infinitely long cellular structure, all the nodes lying along the dashed symmetry line of Fig. 2 (A) or (B) at the top and bottom of the model were connected to a rigid plate. Those nodes were constrained by symmetry conditions, i.e. free to slide left or right, but all maintaining the same y coordinate, and prevented from rotating. This model represents an infinite cellular structure in both in-plane directions and thus, the mechanical response is not dependant on the model size (i.e. eliminating the size effect). We confirmed the independence of the results from the model size by systematically changing the model size from a single unit cell to structure comprising of 8×8 unit cells for a honeycomb with one order hierarchy and relative density of 6% and $\gamma_1 = 0.3$. The unit cell was only 0.5% stiffer than the 8×8 cellular structure (measured by comparing the effective elastic modulus of each system).

In the second set of simulations, those same top and bottom nodes were constrained horizontally by being built into the fixed rigid plates (i.e. tied boundary condition with no rotation and no displacement in the horizontal direction and with equal displacement in the vertical direction for the nodes in contact with the rigid plates), and the side nodes were free as in the experimental setup. In this case, the effective elastic modulus is strongly dependant on the size of the structure. For a model comprising of 5×5 unit cells, which is consistent with our experiments, the increase in modulus caused by this constraint in the second kind of simulation ranged from 3% up to a maximum of about 20% depending on the honeycomb relative density (the different is smaller for honeycombs with lower relative density). Here, we show the numerical results from the first set, which matched the boundary conditions of our analytical model (first model described above for simulating the response of an infinitely long and wide cellular structure). The effective elastic modulus of each structure was calculated from the slope of compressive stress-strain response.

Fig. 3(A) shows the effective elastic modulus of first order hierarchical honeycombs for all possible values of γ_1 . In this fig., the elastic modulus is normalized by the effective stiffness of the counterpart regular honeycomb with the same relative density, $1.5E_s\rho^3$, allowing us to present results for every density on a single curve. In the finite element simulations, structures with three different relative densities (2%, 6% and 10%) were analyzed. Results show quite good agreement between numerical and theoretical approaches, even though the theoretical analysis ignored the axial and shear deformation of the beams (a good approximation only for low density honeycombs with small beam thickness (Harders et al., 2005)). We suspect that the numerical incorporation of shear and stretching accounts for the FEA-determined modulus falling somewhat below the theory, particularly as density increases or beam lengths decrease. The FEA results nicely confirm the near-doubling of stiffness for $\gamma_1 = 0.32$. In this fig., experimental results are also plotted which show reasonable agreement with both theory and numerical

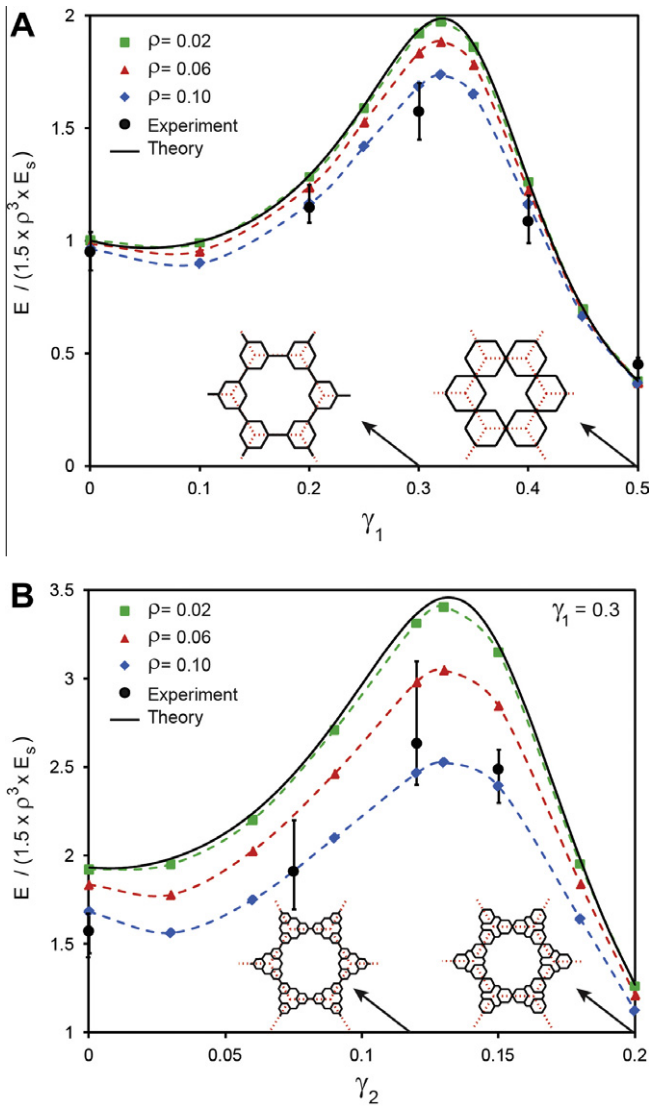


Fig. 3. Stiffness of hierarchical honeycombs. (A) Normalized stiffness for honeycombs with 1st order hierarchy versus γ_1 . (B) Normalized stiffness versus γ_2 , for honeycombs with 2nd order hierarchy and $\gamma_1 = 0.3$. The schematic of the honeycomb unit cells are shown for selected values of γ_1 and γ_2 in each plot. The finite element results are shown for honeycombs with three different relative densities. Experimental results for structures with different hierarchy levels are also shown (black circles). The error bars show the results variation. Each experimental point is from 3 tested specimens.

results. For honeycombs with 2nd order hierarchy, we fixed $\gamma_1 = 0.3$ and plotted the normalized effective elastic modulus for various values of γ_2 . The results again match theory best for low density, and show that honeycombs with two orders of hierarchy where $\gamma_1 = 0.3$, and $\gamma_2 = 0.135$, have stiffness approximately 3.5 times that of regular hexagonal honeycomb with same relative density (i.e. specific stiffness 3.5 times of the regular hexagonal honeycomb).

4. Hierarchical honeycombs: Poisson's ratio

To fully characterize the linear elastic behavior of hierarchical honeycombs, we also need to obtain the dependence of Poisson's ratio, ν , on the dimension ratios. We again used Castigliano's second theorem and considered the same subassemblies under biaxial loading (where the horizontal stress is finally set to zero after differentiating). This is a bending-based approximate analysis that ignores axial and shear deformation of the cell walls.

Temporarily considering horizontal loading only, we apply reasoning similar to that in Section 3, to midpoint cut lines such as L_2 and L_3 . This establishes that the horizontal segment aligned with the dotted line is subjected to pure compression (no bending), and that the segment midpoint to the upper right of each subassembly experiences only a horizontal force. There is no horizontal reaction at node 1 for first order hierarchy, or at nodes 1, 2 for second order hierarchy. But node 2 (first order) and node 3 (second order) has a horizontal reaction to balance $2P$, $-P$, and nodes on the dashed horizontal line still require vertical and moment reactions. The composite free body diagrams for both horizontal and vertical stress are shown in Fig. 2. Fig. 2(A) is for 1st order hierarchy where the external forces P and F are applied at point 4 in x - and y -directions, and N_1 , M_1 , N_2 , and M_2 are the reaction vertical forces and moments at vertices 1 and 2, respectively. The two non-trivial equations of equilibrium (vertical and angular) allow us to write N_2 and M_2 as functions of N_1 , M_1 , P and F . Therefore, the bending energy stored in the subassembly can be expressed as the summation of bending energy in all beams, $U(F, P, M_1, N_1) = \sum \int (M^2 / 2E_s I) ds$, where M is the bending moment at position s along each beam, E_s is the elastic modulus of the cell wall material, and I is the beam's cross sectional area moment of inertia (cell walls are considered to have rectangular cross section with thickness t and unit depth, i.e., $I = t^3 / 12$). The horizontal beam connecting the nodes 2 and 3 can be excluded from the analysis since it experiences no bending moment. Assuming zero displacement and zero rotation at vertices 1 and 2 due to symmetry, one can write $\partial U / \partial N_1 = 0$, and $\partial U / \partial M_1 = 0$. These two relations allow N_1 and M_1 to be calculated as a function of P and F . The bending energy stored in the subassembly can be subsequently expressed as $U = U(F, P)$.

When P is zero (free lateral expansion), the x and y displacements of point 4 due to force F can be expressed as follows, respectively: $\delta_x^F = (\partial U / \partial P)_{P=0}$; $\delta_y^F = (\partial U / \partial F)_{P=0}$. Considering the initial dimensions of the subassembly to be $3a/4$ and $\sqrt{3}a/4$ in X - and Y - dimensions, respectively, the Poisson's ratios in direction Y is obtained as $\nu = \delta_x^F / \sqrt{3} \delta_y^F$, which gives: $\nu = 1 - \gamma_1^3 / (2.9\gamma_1^3 + 3.6\gamma_1^2 - 3.525\gamma_1 + 0.75)$, which is plotted in Fig. 4. The value of ν is $\nu = 1$ at $\gamma_1 = 0$, $\nu = 0.5$ at $\gamma_1 = 0.5$, with the minimum value 0.37 at $\gamma_1 = 0.4$. Finite element results are also shown which were obtained

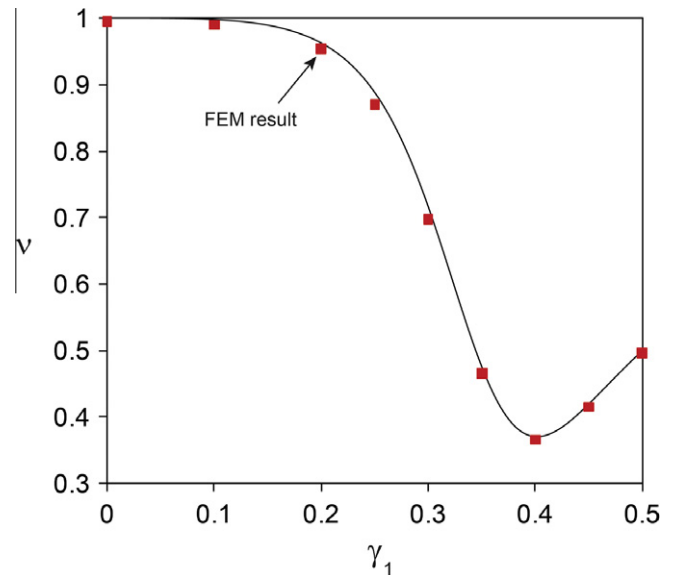


Fig. 4. Poisson's ratio of hierarchical honeycombs with one level of hierarchy versus γ_1 . The finite element results are also plotted for honeycomb with relative density 0.06.

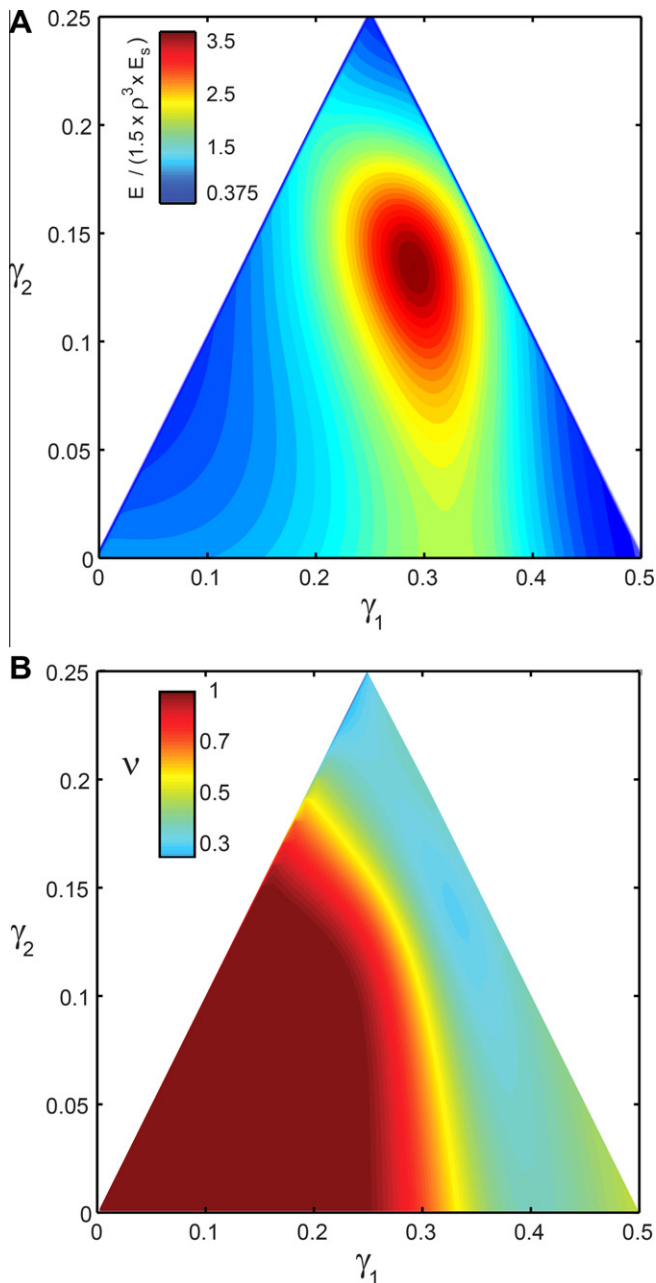


Fig. 5. Contour maps of the (A) effective elastic modulus and (B) Poisson's ratio of hierarchical honeycombs with 2nd order hierarchy for all possible geometries (i.e., admissible range of γ_1 and γ_2).

by calculating the lateral deformation of honeycombs with periodic boundary condition under uniaxial in-plane loading.

For the biaxially loaded 2nd order hierarchical honeycomb subassembly illustrated in Fig. 2(B). N_1 , M_1 , N_2 , M_2 , N_3 , and M_3 are the unknown reaction vertical forces and moments. Once again, vertical and rotational equilibrium equations allow us to write N_3 and M_3 as functions of N_1 , M_1 , N_2 , M_2 , P and F . Therefore, the bending energy stored in the subassembly can be expressed as the summation of bending energy in all beams, $U(F, P, M_1, N_1, M_2, N_2) = \sum \int (M^2/2E_s I) ds$. The horizontal beam connecting nodes 3 and 4 is again excluded from the analysis. Since symmetry prevents vertical displacement or rotation at vertices 1 and 2, one can write $\partial U/\partial N_1 = 0$, $\partial U/\partial M_1 = 0$, $\partial U/\partial N_2 = 0$, and $\partial U/\partial M_2 = 0$. These four relations allow N_1 , N_2 , M_1 and M_2 to be calculated as functions of P and F . The bending energy stored in the

subassembly can be subsequently expressed as $U = U(F, P)$. The x and y displacements of point 5 due to force F can be expressed as: $\delta_x^F = (\partial U/\partial P)|_{P=0}$; $\delta_y^F = (\partial U/\partial F)|_{P=0}$. Considering the initial dimensions of the subassembly to be $3a/4$ and $\sqrt{2}a/4$ in the x and y directions, the Poisson ratio is obtained as: $\nu = \delta_x^F/\sqrt{3}\delta_y^F$. The value of ν ranges from 0.28 at $\gamma_1 = \gamma_2 = 0.23$ to 1.0 at $\gamma_1 = \gamma_2 = 0$.

5. Concluding remarks

To summarize the behavior of all honeycombs with the investigated hierarchical structures, we have plotted contour maps of the effective (normalized) elastic modulus and Poisson's ratio of hierarchical honeycombs with second-order hierarchy for all possible values of γ_1 and γ_2 , as shown in Fig. 5. The x -axis is γ_1 ranges from 0 to 0.5, while γ_2 is limited by the two geometrical constraints, $\gamma_2 \leq \gamma_1$ and $0 \leq \gamma_2 \leq (0.5 - \gamma_1)$. Hierarchical honeycombs with small to moderate values of γ_1 and γ_2 , and especially a simple hexagonal honeycomb, have Poisson ratio near 1.0. This means that the Young's and Shear moduli, which are controlled by element bending, are far lower than the "Bulk" (really, "Areal") modulus which for those structures is controlled by element stretching.

The results show that a relatively broad range of elastic properties, and thus behavior, can be achieved by tailoring the structural organization of hierarchical honeycombs, and more specifically the two dimension ratios. For example, the hierarchical honeycombs with one order and two orders hierarchy are shown to have specific stiffness up to 2.0 and 3.5 times of the regular hexagonal honeycomb. Increasing the level of hierarchy provides a wider range of achievable properties. Further optimization should be possible by also varying the thickness of the hierarchically introduced cell walls, and thus the relative distribution of the mass, between different hierarchy levels. The proposed work focused only on the elastic properties of hierarchical honeycombs, and the collapse/yield and instability properties of these structures are currently under study.

Acknowledgments

The authors thank Drs. John W. Hutchinson and Jerome F. Hajjar for fruitful discussions and Jonathan Doughty, Christopher J. Woodsum and Yoontae Kim for help with the experiments. This work was supported in part by the U.S. Air Force Office of Scientific Research under AFOSR YIP grant award, #FA 9550-10-1-0145 under the technical supervision of Dr. Joycelyn Harrison and in part by the U.S. Department of Homeland Security under Award Number 2008-ST-061-ED0001. The views and conclusions contained in this document are those of the authors and should not be interpreted as necessarily representing the official policies, either expressed or implied, of the U.S. Department of Homeland Security.

References

- Aizenberg, J., Weaver, J.C., Thanawala, M.S., Sundar, V.C., Morse, D.E., Fratzl, P., 2005. Skeleton of euleptella sp.: structural hierarchy from the nanoscale to the macroscale. *Science* 309, 275–278.
- Ajdari, A., Nayeb-Hashemi, H., Vaziri, A., 2011. Dynamic crushing and energy absorption of regular, irregular and functionally graded cellular structures. *Int. J. Solids Struct.* 48, 506–516.
- Bhat, T., Wang, T.G., Gibson, L.J., 1989. Micro-Sandwich Honeycomb. *SAMPE* 25, 43–45.
- Boresi, A.P., Schmidt, R.J., 2002. *Advanced Mechanics of Materials*. Wiley.
- Buehler, M.J., 2006. Nature designs tough collagen: explaining the nanostructure of collagen fibrils. *Proc. Nat. Acad. Sci.* 103, 12285–12290.
- Burgueño, R., Quagliata, M.J., Mohanty, A.K., Mehta, G., Drzal, L.T., Misra, M., 2005. Hierarchical cellular designs for load-bearing biocomposite beams and plates. *Mater. Sci. Eng., A* 390, 178–187.
- Christensen, R.M., 1987. Sufficient symmetry conditions for isotropy of the elastic moduli tensor. *J. Appl. Mech.* 54, 772–777.
- Chuang, C.-H., Huang, J.-S., 2002a. Effects of solid distribution on the elastic buckling of honeycombs. *Int. J. Mech. Sci.* 44, 1429–1443.

- Chuang, C.-H., Huang, J.-S., 2002b. Elastic moduli and plastic collapse strength of hexagonal honeycombs with plateau borders. *Int. J. Mech. Sci.* 44, 1827–1844.
- Cote, F., Russell, B.P., Deshpande, V.S., Fleck, N.A., 2009. The through-thickness compressive strength of a composite sandwich panel with a hierarchical square honeycomb sandwich core. *J. Appl. Mech.* 76, 061004–061008.
- Espinosa, H.D., Juster, A.L., Latourte, F.J., Loh, O.Y., Gregoire, D., Zavattieri, P.D., 2011. Tablet-level origin of toughening in abalone shells and translation to synthetic composite materials. *Nature Communication* 2, 173.
- Fan, H.L., Jin, F.N., Fang, D.N., 2008. Mechanical properties of hierarchical cellular materials. Part I: Analysis. *Compos. Sci. Technol.* 68, 3380–3387.
- Fratzl, P., Weinkamer, R., 2007. Nature's hierarchical materials. *Prog. Mater. Sci.* 52, 1263–1334.
- Gibson, L.J., Ashby, M.F., Harley, B.A., 2010. *Cellular Materials in Nature and Medicine*. Cambridge University Press.
- Gibson, L.J., Ashby, M.F., 1997. *Cellular Solids: Structures and Properties*, second ed. Cambridge University Press, Cambridge.
- Harders, H., Hupfer, K., Rösler, J., 2005. Influence of cell wall shape and density on the mechanical behaviour of 2D foam structures. *Acta Mater.* 53, 1335–1345.
- Kazemahvazi, S., Tanner, D., Zenkert, D., 2009. Corrugated all-composite sandwich structures. Part 2: Failure mechanisms and experimental programme. *Compos. Sci. Technol.* 69, 920–925.
- Kazemahvazi, S., Zenkert, D., 2009. Corrugated all-composite sandwich structures. Part 1: Modeling. *Compos. Sci. Technol.* 69, 913–919.
- Kooistra, G.W., Deshpande, V., Wadley, H.N.G., 2007. Hierarchical Corrugated Core Sandwich Panel Concepts. *J. Appl. Mech.* 74, 259–268.
- Lakes, R., 1993. Materials with structural hierarchy. *Nature* 361, 511–515.
- Lu, T.J., Chen, C., 1999. Thermal transport and fire retardance properties of cellular aluminium alloys. *Acta Mater.* 47, 1469–1485.
- Murphey, T., Hinkle, J., 2003. *Some Performance Trends in Hierarchical Truss Structures*. AIAA, Norfolk, VA, p. 1903.
- Ortiz, C., Boyce, M.C., 2008. Bioinspired Structural Materials. *Science* 319, 1053–1054.
- Qing, H., Mishnaevsky Jr, L., 2009. 3D hierarchical computational model of wood as a cellular material with fibril reinforced, heterogeneous multiple layers. *Mech. Mater.* 41, 1034–1049.
- Rathbun, H.J., Radford, D.D., Xue, Z., He, M.Y., Yang, J., Deshpande, V., Fleck, N.A., Hutchinson, J.W., Zok, F.W., Evans, A.G., 2006. Performance of metallic honeycomb-core sandwich beams under shock loading. *Int. J. Solids Struct.* 43, 1746–1763.
- Simone, A.E., Gibson, L.J., 1998. Effects of solid distribution on the stiffness and strength of metallic foams. *Acta Mater.* 46, 2139–2150.
- Taylor, C.M., Smith, C.W., Miller, W., Evans, K.E., 2011. The effects of hierarchy on the in-plane elastic properties of honeycombs. *Int. J. Solids Struct.* 48, 1330–1339.
- Vaziri, A., Hutchinson, J.W., 2007. Metal sandwich plates subject to intense air shocks. *Int. J. Solids Struct.* 44, 2021–2035.
- Vaziri, A., Xue, Z., Hutchinson, J.W., 2007. Performance and failure of metal sandwich plates subject to shock loading. *J. Mechanics of Materials and Structures* 2, 1947–1964.
- Vaziri, A., Xue, Z., Hutchinson, J.W., 2006. Metal sandwich plates with polymeric foam-filled cores. *J. Mechanics of Materials and Structures* 1, 95–128.
- Vaziri, A., Xue, Z., 2007. Mechanical behavior and constitutive modeling of metal cores. *J. Mech. Mater. Struct.* 2, 1743–1760.
- Wadley, H., Dharmasena, K., Queheillalt, D., Chen, Y.C., Dudt, P., Knight, D., Xue, Z., Vaziri, A., 2007. Dynamic crushing of square honeycomb structures during underwater impulsive loading. *J. Mechanics of Materials and Structures* 2, 2025–2048.
- Xue, Z., Hutchinson, J.W., 2004. A Comparative study of impulse-resistant metal sandwich plates. *Int. J. Impact Eng.* 30, 1283–1305.
- Xue, Z., Hutchinson, J.W., 2006. Crush dynamics of square honeycomb sandwich cores. *Int. J. Numer. Meth. Eng.* 65, 2221–2245.
- Zheng, Z., Yu, J., Li, J., 2005. Dynamic crushing of 2D cellular structures: A finite element study. *Int. J. Impact Eng.* 32, 650–664.